Multidirectional observation of an embedded quantum dot

Kita, Takashi ; Inoue, Tomoya ; Wada, Osamu ; Konno, Mitsuru ; Yaguchi, Toshie ; Kamino, Takeo

(Citation)
Applied Physics Letters,90(4):41911-41911

(Issue Date)
2007-01

(Resource Type)
journal article

(Version)
Version of Record

(URL)
https://hdl.handle.net/20.500.14094/90000189

Multidirectional observation of an embedded quantum dot

Takashi Kita,[a] Tomoya Inoue, and Osamu Wada
Faculty of Engineering, Department of Electrical and Electronics Engineering, Kobe University, 1-1 Rokkodai, Nada, Kobe 657-8501, Japan

Mitsuru Konno, Toshie Yaguchi, and Takeo Kamino
Nanotechnology Products Business Group, Hitachi High-Technologies Corporation, 1-1 Ishikawa, Hitachinaka, Ibaraki 312-0057, Japan

(Received 14 November 2006; accepted 21 December 2006; published online 24 January 2007)

The authors succeeded in observing atomic scale images of undamaged single InAs quantum dots (QDs) embedded in the GaAs matrix using high resolution transmission electron microscope equipped with focused ion beam system. The QD can be viewed from multidirections, and a conclusive and comprehensible determination of the size and the shape anisotropy has been realized. Asymmetry of the structural properties has been confirmed between the [110] and [−110] crystal directions. The embedded QD is elongated along the [−110] axis. The strain-field pattern is also asymmetric according to the shape anisotropy. The results will enable the investigation of the exact structure anisotropy influencing the atomlike properties of QDs. © *2007 American Institute of Physics*. [DOI: 10.1063/1.2436633]

Atomlike electronic states of self-assembled semiconductor quantum dots (QDs) produce excellent functions for quantum information applications. Especially, the radiative decay of biexcitons in a QD is expected as a source of event-ready polarization entangled photon pairs.[1–6] However, the two intermediate exciton states in real QDs are nondegenerate because of in-plane asymmetries of the structural properties of the QD.[7–10] The fine-structure splitting of the intermediate states gives rise to the "which path" information. Generally, the QD is elongated along the [−110] crystal axis, which comes from the nature of the self-assembled epitaxial growth.[11–13] The atomistic asymmetry and the in-built piezoelectric field cause the anisotropic optical transitions for the [110] and [−110] polarizations. According to abundant photoluminescence measurements of single QDs in a QD ensemble, a relative trend between the splitting and the recombination energy has been evaluated.[2,3] However, the obtained results do not show a unified trend, which sensitively depends on the growth condition. In order to control the fine-structure splitting, the in-plane symmetry of embedded QDs still needs to be clarified. In particular, the anisotropy between [110] and [−110] is important. For this purpose, we have to perform the direct observation for single QDs embedded in the matrix and to investigate the structural properties. The result will enable us to optimize growth strategies for QDs.

Although the shape of *uncapped* QDs is easy to observe by *in situ* scanning-tunneling microscopy (STM),[11–13] the dot structure is not necessarily the same as that embedded in a matrix because of In segregation during the capping layer growth. Recently, a cross-sectional STM technique has been developed to investigate the real-space image of single QDs embedded in a GaAs matrix.[14] This measurement is expected to determine the shape, size, and composition of the QDs. However, the image depends on the cleavage plane, and furthermore, it is impossible to observe the single QD from multidirections. Conventional cross-sectional transmission electron microscopy (TEM) also has the same problem. Here we conceptually advanced the TEM technology by combining with the focused ion beam (FIB) microsampling technique[15] and succeeded in observing multidirectional high resolution TEM images of single InAs QDs embedded in GaAs. A single QD is selected and extracted from a desired portion of the epitaxial wafer. The QD is placed at the center of a micropillar. The multidirectional TEM observation reveals the anisotropic structural properties. Furthermore, this technique can realize an extremely precise fabrication process of micropillar devices including a desired single QD.

Self-assembled InAs QDs were grown on GaAs(001) substrates by solid-source molecular beam epitaxy. The As pressure was kept constant at 3.0×10^{-6} Torr beam equivalent pressure. InAs was deposited at 460 °C after growing a 510 nm thick GaAs-buffer layer. The growth rate was 0.012 ML/s. The deposited nominal thickness of InAs was 3.6 ML. The QD size can be controlled by changing the deposited thickness and the growth rate. In the lattice-mismatched system of (In,Ga)As/GaAs, the self-assembled growth can be achieved by the Stranski-Krastanov growth mode.[16] Above the critical thickness of about 1.8 ML, the growth mode is transformed from the two-dimensional layer-by-layer growth to the three-dimensional island growth. The growth-mode transition is determined from the change in the reflection high-energy electron diffraction (RHEED) pattern. At the growth transition, the RHEED exhibits chevron patterns representing the QD formation. After growing the InAs QDs, the dots were capped by a 150 nm thick GaAs.

After milling to a size of approximately 300×300 nm^2, we select a single QD for the three-dimensional TEM observation. This procedure is shown in Fig. 1. TEM images observed with the incident beam parallel to the [110] and [−110] directions are displayed on the right of the illustration indicating the size and the crystal axes. The black image at the topmost layer is a tungsten layer.[15] Formation of an about 20 nm thick wall of amorphous GaAs during the FIB process is confirmed. Figure 1(a) displays the initial pillar structure with the size of about 320×290 nm^2. As shown in Fig. 1(b),

[a]Electronic mail: kita@eedept.kobe-u.ac.jp

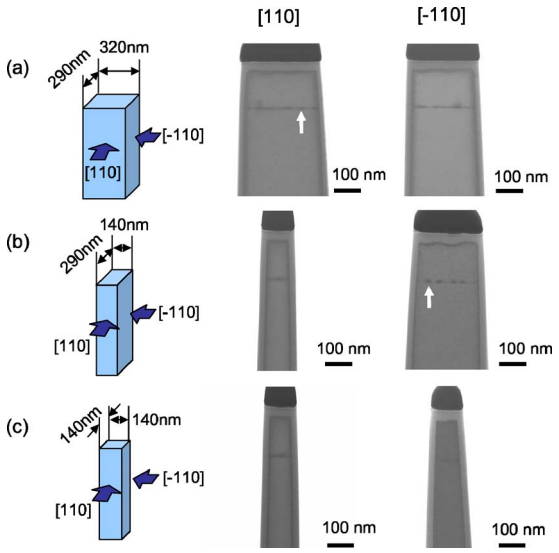

FIG. 1. (Color online) FIB sampling process. (a) TEM images observed with the incident beam parallel to the [110] and [−110] directions are listed on the right of the illustration. The black image at the topmost layer is a tungsten layer. An about 20 nm thick amorphous GaAs wall is formed by the FIB process. The size of the initial pillar structure is about $320 \times 290\ \mathrm{nm}^2$. (b) The width along the [−110] direction is reduced by the FIB after a desired dot is selected (white arrow). (c) Next, the width along the [110] direction is reduced in order to extract the single dot.

the width along the [−110] direction is reduced by the FIB after a desired dot is selected. Next, the width along the [110] direction is reduced in order to extract the single dot [Fig. 1(c)]. Thus the position of the QD in the pillar can be controlled precisely by the *in situ* FIB process. Finally, the pillar sample is milled gently using 500 eV Ga^+ ions to reduce the damaged layer, which enables to obtain clearer lattice images. Figures 2(a) and 2(b) show TEM images of the finally milled pillar sample observed with the incident beam parallel to the [110] and [−110] directions, respectively. The selected single QD is confirmed to be placed at the center of the pillar sample. The size of the pillar sample is reduced to about $80 \times 80\ \mathrm{nm}^2$ and the thickness of the damaged layer is dramatically reduced to about 5 nm. Multidirectional high resolution TEM observation can be accomplished using this pillar sample.

High resolution TEM images of the pillar sample have been observed with the incident beam parallel to the [110] [Fig. 2(c)] and [−110] [Fig. 2(d)] directions. The observed direction has been adjusted precisely by confirming the electron-beam diffraction pattern as show in the inset of Figs. 2(a) and 2(b). The lattice fringes of the (111) plane of GaAs are clearly observed as magnified in Fig. 2(d), which has been attained by the final gentle milling. The embedded QD observed from both directions has been revealed to have in-plane asymmetry in size and shape. Although a faint strain-field contrast overlaps with the lattice image, the asymmetry is appreciable. The QD is confirmed to be elongated along the [−110] crystal axis. The height is about 5 nm, and the base lengths are about 21 and 23 nm along [110] and [−110], respectively. These scales are almost the same as the values for uncapped QDs measured by STM.[13] The shape anisotropy depending on the base length is considered to come from the anisotropic formation of the crystal facets between these directions. Generally, the low index facets such as (111) and (−1−11) are known to form preferentially

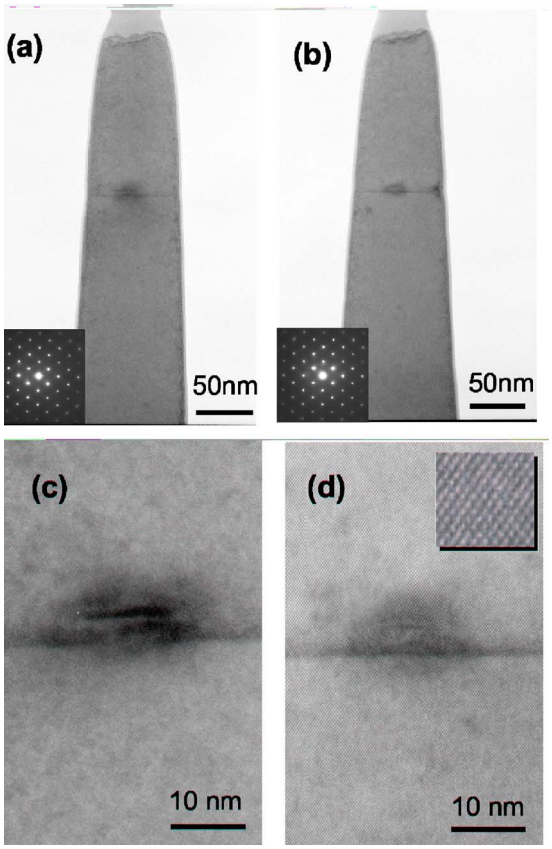

FIG. 2. Multidirectional TEM images of a single QD placed at the center of a micropillar. Low-magnification TEM images of the pillar sample observed with the incident beam parallel to the [110] and [−110] directions are shown in (a) and (b), respectively. (c) and (d) are high resolution TEM images corresponding to (a) and (b), respectively.

at the final stage of the QD growth.[12,13] The relatively low growth rate of the low index faceted planes gives rise to the anisotropic shape. The facet interfaces between the QD and the capping layer are unclear because of the In segregation during the capping layer growth. Furthermore, it is found that the strain-field pattern is asymmetric according to the shape anisotropy. The shape anisotropy and the resultant anisotropic strain distribution provide key factors for understanding the excitonic states.

The strain-field contrast seems to be remarkable in the image taken at the electron-beam incident azimuth along the [110] direction [Fig. 2(c)]. This may indicate that the strain distribution is preferential along the [−110] direction, i.e., the long axis of the QD. Actually, for an almost isotropic QD, such anisotropic strain contrast has been found to be weak. However, as can be seen from the diffraction patterns in Fig. 2, the crystal orientations are both slightly off the corresponding zone axes. Figure 2(a) shows that the sample has been tilted slightly about the [001] axis and just a little about [−110], as the diffraction spots are somewhat more intense towards the bottom right. This tilt is very small, however, and the strong strain observed is due to the near-zone-axis orientation. In Fig. 2(b) the sample is tilted about the [110] axis, as the top diffraction spots are brighter than the lower ones. This tilt implies that the interface structure is not viewed edge-on, reducing the overall strain contrast. As the strain extends further out of the quantum dot into the surrounding material, a zone-axis orientation with lots of strain contrast will automatically show a larger structure while a

quantum dot will appear smaller if imaged under slight off-axis conditions that suppress strain contrast. These facts caused by the slight tilt are considered to be insignificant but cannot be denied completely.

In conclusion, the multidirectional observation reveals the anisotropic structural properties of the embedded QD, which has never been observed. By comparing multidirectional TEM images of QDs grown at different growth conditions, we will be able to optimize growth strategies for QDs with isotropic structural properties. The developed FIB-TEM technique is applicable to any material which can be processed by the FIB and would be a powerful tool to investigate the solid image of desired materials. That strategy represents a significant conceptual advantage in the field of electron microscopy. On the other hand, the *in situ* FIB process is also expected to be useful in fabricating precisely single QD devices.

[1]O. Benson, C. Santori, M. Pelton, and Y. Yamamoto, Phys. Rev. Lett. **84**, 2513 (2000).
[2]R. J. Young, R. M. Stevenson, A. J. Shields, P. Atkinson, K. Cooper, D. A. Ritchie, K. M. Groom, A. I. Tartakovskii, and M. S. Skolnick, Phys. Rev. B **72**, 113305 (2005).
[3]R. Seguin, A. Schliwa, S. Rodt, K. Poetschke, U. W. Pohl, and D. Bimberg, Phys. Rev. Lett. **96**, 257402 (2005).
[4]R. M. Stevenson, R. J. Young, P. See, D. G. Gevaux, K. Cooper, P. Atkinson, I. Farrer, D. A. Ritchie, and A. J. Shields, Phys. Rev. B **73**, 033306 (2006).
[5]R. M. Stevenson, R. J. Young, P. Atkinson, K. Cooper, D. A. Ritchie, and A. J. Shields, Nature (London) **439**, 179 (2006).
[6]N. Akopian, N. H. Lndner, E. Poem, Y. Berlatzky, J. Avron, D. Gershni, B. D. Gerardot, and P. M. Petroff, Phys. Rev. Lett. **96**, 130501 (2006).
[7]V. D. Kulakovskii, G. Bacher, R. Weigand, T. Kümmell, A. Forchel, E. Borovitskaya, K. Leonardi, and D. Hommel, Phys. Rev. Lett. **82**, 1780 (1999).
[8]L. Besombes, K. Kheng, and D. Martrou, Phys. Rev. Lett. **85**, 425 (2000).
[9]R. M. Stevenson, R. M. Thompson, A. J. Shields, I. Farrer, B. E. Kardynal, D. A. Ritchie, and M. Pepper, Phys. Rev. B **66**, 081302(R) (2002).
[10]J. Persson, M. Holm, and C. Pryor, Phys. Rev. B **67**, 035320 (2003).
[11]Y. Hasegawa, H. Kiyama, Q. K. Xue, and T. Sakurai, Appl. Phys. Lett. **72**, 2265 (1998).
[12]B. A. Joyce, T. S. Jones, and J. G. Belk, J. Vac. Sci. Technol. B **16**, 2373 (1998).
[13]M. C. Xu, Y. Temko, T. Suzuki, and K. Jacobi, J. Appl. Phys. **98**, 083525 (2005).
[14]D. M. Bruls, J. W. A. M. Vugs, P. M. Koenraad, H. W. M. Salemink, J. H. Wolter, M. Hopkinson, M. S. Skolnick, Fei Long, and S. P. A. Gill, Appl. Phys. Lett. **81**, 1708 (2002).
[15]T. Kamino, T. Yaguchi, M. Konno, T. Ohnishi, and T. Ishitani, J. Electron Microsc. **53**, 583 (2004).
[16]B. A. Joyce and D. D. Vvedensky, Mater. Sci. Eng., R. **46**, 127 (2004).